

Coarsening Mechanisms in a Metal Film: From Cluster Diffusion to Vacancy Ripening

J.-M. Wen, J. W. Evans, M. C. Bartelt, J. W. Burnett,* and P. A. Thiel

Departments of Chemistry and Mathematics, and Ames Laboratory, Iowa State University, Ames, Iowa 50011

(Received 17 April 1995)

Coarsening of Ag films on Ag(100) at room temperature occurs primarily via diffusion-mediated coalescence of two-dimensional adatom clusters, rather than by Ostwald ripening, up to a coverage of 0.65 monolayer. Above 0.8 monolayer, vacancy clusters coarsen primarily via Ostwald ripening, due to their much lower diffusivity. An asymmetric transition region separates these two regimes, characterized by a near-percolating structure which undergoes self-similar coarsening.

PACS numbers: 68.35.Fx, 61.16.Ch, 66.30.Fq, 68.60.-p

The evolution and control of film morphology is of fundamental and technological interest. Typically, during deposition a film is driven far from equilibrium, and thus can be potentially “trapped” in a variety of manifestly nonequilibrium configurations [1–3]. While this allows control of morphology by intelligent manipulation of deposition parameters, one must recognize that a nonequilibrium structure is always prone to rearrangement. Understanding the mechanisms and kinetics of such rearrangement is necessary to predict film stability, and presents a key challenge in nonequilibrium physics.

Below a critical temperature for two-dimensional (2D) phase separation, the equilibrium structure of a partially filled layer consists of a single large domain or “island” of a condensed phase coexisting with a dilute 2D gas phase [4]. Since nucleation and growth of islands during deposition produces a distribution of “smaller” islands [5,6], *subsequent* temporal evolution toward the equilibrium state must involve coarsening, i.e., an increase in the length-scale characteristic of the dominant structure [7]. Current discussions of coarsening in adlayers primarily invoke Ostwald ripening (OR) [7,8], at least for low coverages, θ . During OR, atoms tend to detach from smaller islands and reattach to larger islands, driven by a gradient in the vapor pressure of the surrounding 2D gas. This process results in asymptotically self-similar growth, with the characteristic linear dimension L increasing with time as $L \sim t^{1/3}$ (the Lifshitz-Slyozov law) [9]. It has also been recognized that another mechanism can control coarsening at moderate θ , where the adlayer has an interconnected and interpenetrating structure [8]. This is the edge running mechanism, which involves long-range diffusion of adatoms along the domain boundary of the condensed phase.

A substantial body of generic 2D lattice-gas modeling of coarsening phenomena exists [10], which might be expected to apply to adlayer evolution. However, in the absence of information on activation barriers for adatom hopping rates in various configurations, these studies invariably use simple Metropolis or Kawasaki rate choices [10]. While this approach might reasonably describe equilibrium behavior (for a suitably chosen Hamiltonian), it cannot correctly predict competition between different kinetic pathways during coarsening of nonequilibrium structures.

The primary goal here is to determine the coarsening mechanism and kinetics for various θ , for Ag/Ag(100) at 300 K. This is the first comprehensive analysis of adlayer coarsening in such a system. We are even able to assess the *relative* contributions to coarsening of OR and a competing mechanism, cluster diffusion (CD) and subsequent coalescence, *both* for adatom clusters at low θ and for vacancy clusters at high θ . While CD was recognized in older studies of coarsening of 3D metal (adatom) clusters on nonmetallic surfaces [11,12], it has been overlooked in 2D metal-on-metal systems, presumably because of an expectation that diffusion of large 2D adatom or vacancy clusters is insignificant. Previously, the coarsening of vacancy islands has received only cursory attention [13,14]. We find, in fact, that CD of adatom islands dominates coarsening for low θ , and present detailed modeling of this behavior. A dramatic asymmetry between behavior at low and high θ is revealed. We also determine the transition region where interconnected domains, necessary to support edge running, occur, and apply appropriate concepts from correlated percolation theory to explain why this region occurs well above 0.5 monolayer (ML).

Scanning tunneling microscopy (STM) allows *direct* determination of the mechanism of coarsening (see Fig. 1). We use an Omicron STM housed in a UHV chamber, as described previously [15]. Evaporation of submonolayer coverages, with the sample held at room temperature, generates the “initial” nonequilibrium 2D structures, whose features are then monitored quantitatively as a function of time, to observe coarsening over a period of several hours. Precautions are taken to eliminate tip-induced effects [15].

The nucleation, growth, and subsequent coalescence of 2D islands during deposition is fairly well understood [5]. Nucleation of stable islands occurs only at very low θ , after which existing islands grow, and the island density per unit area N remains constant until the onset of growth-induced coalescence around 0.4 ML. Percolation occurs much later, around 0.7–0.8 ML [6]. We can tailor the initial configuration created by deposition, simply by changing the deposition flux R : At fixed θ and temperature, N decreases, and the mean island area or size, $S_{av} \approx \theta/N$, increases with decreasing R . For the low θ (adatom island) regime, we label this initial configuration only with θ

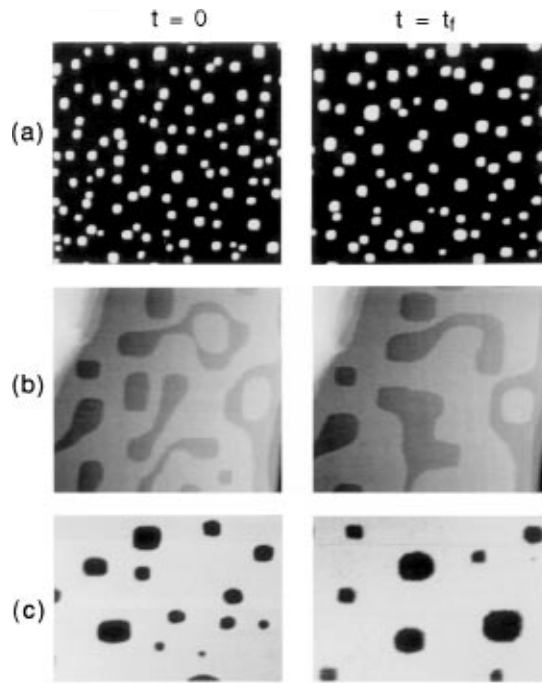


FIG. 1. STM images obtained following deposition of Ag on Ag(100) at room temperature. In each row, the left frame shows the starting point, and the right frame shows the surface several hours later. Full horizontal scale is 1500 Å. Bright areas are the deposited film, one atom deep; dark areas are substrate. Each frame shows a single terrace of the substrate, except (b) where bunched steps are visible at the edges. Conditions are (a) 0.11 ML, $N_0 = 4.9 \times 10^{-5} \text{ \AA}^{-2}$, $t_f = 520$ min; (b) 0.69 ML, $t_f = 400$ min; and (c) 0.87 ML, $N_0 = 1.5 \times 10^{-5} \text{ \AA}^{-2}$, $t_f = 390$ min. N_0 is the initial island density.

and S_{av} (or, equivalently, θ and N), although the full size and separation distributions provide a more complete description. A similar prescription applies to the high θ (vacancy cluster) regime. In the transition range of θ , where the film constitutes a near-percolating network, an appropriate measure of characteristic linear dimension is the mean chord length or terrace length (in a specified direction).

We now examine experimental data for coarsening in the three different θ regimes. The *low- θ (adatom-island) regime* illustrated in Fig. 1(a) encompasses the majority of the first layer, since it extends up to about 0.65 ML. Here, we choose four initial configurations, labeled α – δ in Fig. 2(a), and show N vs t for each point in Fig. 2(b). In each case, the total decrease in N is broken down into two components: one due to OR, and one due to CD (each component representing N values that would occur if only one of the coarsening mechanisms was active). The contribution of each is determined directly from the STM images. OR is taken to occur when a cluster disappears without an obvious collision, and also without a marked increase in size of any single neighbor. This is often preceded by a gradual shrinkage. CD, on the other hand, can usually be discerned clearly by following the clusters' trajectories, and by confirming the growth of a single

neighbor when a cluster disappears. (A cluster which disappears via OR contributes to the minuscule growth of several neighbors.) Also, after collision, the overlapping, near-square shapes of the two original clusters sometimes remain visible for a time. By applying these criteria in examining the STM images, there is an ambiguity in determining the mechanism of cluster disappearance in $<5\%$ of cases.

Surprisingly, in the entire low- θ region, coarsening is dominated by CD, rather than by the traditionally pictured OR. Focusing on the part of this regime specified by Fig. 2(a), for instance, OR is insignificant at the two points, α and β , which are characterized by *large* S_{av} . OR is measurable for both the *lower* S_{av} points, γ and δ , but even there it only competes significantly with CD at δ . See Fig. 2(b).

These are reasonable observations, given the recent discovery [15] that large 2D adatom islands on Ag(100) undergo significant diffusion at 300 K on the time scale of equilibration. Within a range of island sizes S of 100–700 atoms, the diffusion coefficient $D \approx 10^{-17} \text{ cm}^2 \text{ s}^{-1}$ varies little with island size (by a factor of 2 at most), suggesting that cluster diffusion is dominated by evaporation-condensation (EC) processes [15]. Given the weak dependence of D on S , one expects that increasing the average initial island size [e.g., going from γ – δ to α – β in Fig. 2(a)] does not diminish the effectiveness of the CD process. However, absolute rates for island shrinkage

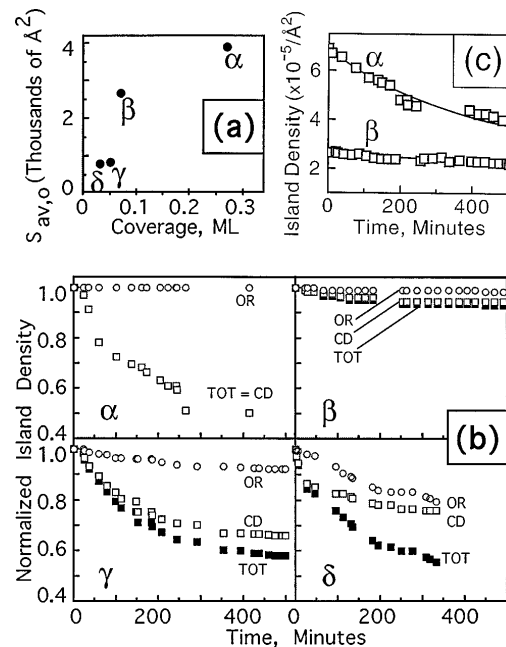


FIG. 2. Coarsening in the low-coverage regime. (a) The size-coverage space spanned by the four points studied. Initial conditions are (α) 0.27 ML, $N_0 = 6.7 \times 10^{-5} \text{ \AA}^{-2}$; (β) 0.07 ML, $N_0 = 2.6 \times 10^{-5} \text{ \AA}^{-2}$; (γ) 0.05 ML, $N_0 = 5.8 \times 10^{-5} \text{ \AA}^{-2}$; (δ) 0.03 ML, $N_0 = 3.7 \times 10^{-5} \text{ \AA}^{-2}$. (b) Island densities as functions of time, for the four data points in (a), normalized to the initial density. (c) Rate-equation results (solid lines) for data corresponding to α and β .

or growth decrease as the mean curvature increases, and thus OR is inhibited for the larger S_{av} [7]. It might seem contradictory that CD prevails over OR, since the EC mechanism dominating cluster diffusion is also the basic atomic mechanism underlying OR. However, significant cluster motion via EC events can occur with little change in cluster size, if there is a high probability of recondensation (at the same cluster) after each evaporation event.

A second factor, which also determines the propensity for CD, is the average separation between neighboring islands. This is the main quantity which varies within each pair of data points at roughly constant S_{av} , α and β , or γ and δ , in Fig. 2. The average separation between island centers is given by $L_{av} = N^{-1/2}$, and that between edges by $L_e = (1 - \theta^{1/2})L_{av} = (\theta^{-1/2} - 1)S_{av}^{1/2}$. For instance, in going from α to β , L_e increases from 60 to 145 Å. Since island edges are much closer in α , clusters need diffuse a shorter distance before they touch, and it is reasonable that CD is more efficient than at β . Similarly, for the two points at lower S_{av} , the value of L_e is smaller at γ (100 Å) than at δ (135 Å), which explains why CD is more significant at γ than at δ . In short, CD is the dominant coarsening mechanism in the entire low- θ regime, except in the extreme limits of low θ (thus low S_{av}) and large separation between islands.

More quantitative insight is provided by a rate equation analysis. Analyses of diffusion-mediated “coagulation” processes date back to the work of Smoluchowski [16], where evolution of the density per unit area N_k of islands of size k is described by the infinite coupled set of equations

$$dN_k/dt = (1/2) \sum_{i+j=k} W_{ij} - \sum_i W_{ik}. \quad (1)$$

The collision rate W_{ik} for clusters of size i and k is traditionally chosen as $W_{ik} \approx DN_i N_k$, for size-independent D . However, Eq. (1)—and its recent refinements [17,18]—fail to account for the θ dependence between, for instance, points α and β in Fig. 2(a). This is because Eq. (1) does not take into account the effective size or edge separation of the clusters. In order to correct this, we write the collision rates as $W_{ik} \sim P_k N_i / \tau$, where τ is the time for the i cluster to diffuse to a neighboring cluster, and $P_k = N_k / N$ is the probability that a neighboring cluster is of type k . The relative motion of clusters i and k is described by a space-filling random walk with diffusion coefficient $2D$, and for them to meet, this walk must scan $\sim a^{-2} L_e^2$ sites. Here a is the separation between adjacent adsorption sites. This takes an average time [19] $\tau \sim (L_e^2 / \pi) \ln(a^{-2} L_e^2 / \pi) / 2D$, yielding $W_{ik} \sim DN_i N_k / (1 - \theta^{1/2})^2$ neglecting \ln corrections.

These equations, with the measured average value of $D \approx 2 \times 10^{-17} \text{ cm}^2 \text{ s}^{-1}$ and the measured initial island size distribution as input, provide a parameter-free determination of the time evolution of $N = \sum_k N_k$. The solid lines in Fig. 2(c) show results for points α and β . (We do not attempt to fit points γ or δ , since OR is signifi-

cant there.) The excellent agreement between model and experiment provides additional support for the claim that cluster coalescence is the dominant mechanism of coarsening under these conditions. More importantly, it indicates that knowledge of D leads to reliable, quantitative predictions of coarsening kinetics.

The data do not display the asymptotic decay, $N \sim 1/t$, and exponential size distributions predicted by the classic theories [17,18]. This can be explained in terms of a characteristic time, $t_c = |d \ln N / dt|^{-1}$ (evaluated at $t = 0$), for the coarsening process, which indicates the time for N to decrease by a fixed fraction (by $1/e$ for exponential decay). t_c can be calculated precisely from Eq. (1) and the initial size distribution, but is given effectively by $t_c \approx (1 - \theta^{1/2})^2 / DN$ which varies from ~ 7 h for point α to ~ 30 h for point β . This is comparable to the duration of experimental observation, explaining why asymptotic behavior has not yet appeared.

We have also monitored the evolution of the full island size distribution. For OR, one would expect sharpening of the initial distribution produced by the nucleation process because of a natural evolution toward equal sizes and a corresponding slowdown in coarsening [7]. Instead, the data, e.g., for point α up to 8 h, shows broadening consistent with evolution to a monotonically (exponentially) decreasing form. Evolution to such a form is predicted by the rate equation theory [17,18], and is observed by evolving Eq. (1) for longer times (e.g., 20–40 h for point α). (While the experiment could have been continued longer, statistics of the island distribution become progressively poorer.) The feature that CD produces much broader size distributions than OR can be important if one wishes to use coarsening to tailor size distributions.

One might expect a mirror symmetry in the coarsening mechanism and kinetics between, say, adatom islands at $\theta \approx 0.1$ and vacancy islands at $\theta \approx 0.9$. Thus, we also examine the *high- θ regime* of well-defined, separated vacancy islands, which extends above ca. 0.80 ML. Here, deposition produces adatom islands sharing so many borders that the film percolates, i.e., it produces a contiguous adlayer pockmarked by isolated vacancy regions. These resulting vacancies are mostly compact, and roughly square [Fig. 1(c)]. (Although the vacancies formed during deposition are more irregular [6], most of them must restructure quickly between the end of deposition and the start of imaging, roughly 15 min.) At these θ , a few second-layer adatom islands are usually observable after deposition. With time, the second-layer islands disappear and partially fill in the vacancies [20], leaving a surface layer consisting of isolated vacancy islands. This we take as the starting point to examine coarsening of the vacancies, as shown in Fig. 1(c).

This examination reveals two related asymmetries between the low- θ and high- θ regimes. First, the vacancy islands diffuse more slowly than do their mirror-image adatom islands. This is borne out by a quantitative evaluation of D for vacancy islands at 300 K, which is an

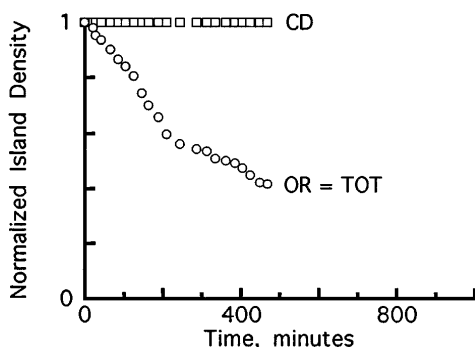


FIG. 3. $N(t)$ for vacancy clusters at $\theta = 0.87$, $N_0 = 1.5 \times 10^{-5} \text{ \AA}^{-2}$. Note that the initial average vacancy island size is about twice that of the adatom islands in α .

order of magnitude lower than for the adatom islands, i.e., $3 \times 10^{-18} \text{ cm}^2 \text{ s}^{-1}$. This value varies little as a function of size in a range of 350–3800 atomic vacancies. (See Ref. [20] for more details.) The second asymmetry is in the coarsening mechanism. Given that D is so much smaller, cluster diffusion was not expected to play as important a role as at lower θ . This is borne out by the data in Fig. 3 showing the decrease in the vacancy island density as a function of time, at $\theta = 0.87$. Vacancy cluster collisions are simply never observed. Coarsening is due solely to OR of the vacancies. This “particle-hole” inequivalence between coverages θ and $1 - \theta$ reflects an asymmetry in associated microscopic activation barriers [20].

Finally, the *transition between the regimes of adatom islands and vacancy islands* extends from about 0.65 to 0.80 ML. In this regime, extensive linkage of adatom islands during deposition leads to a ramified network which percolates at about 0.8 ML. This “continuum percolation” threshold is elevated above the typical value of 0.7 ML due to an effective long-range repulsion between islands formed during deposition, which inhibits percolation [6]. Below about 0.65 ML, we have observed that any small ramified clusters of islands restructure to compact forms, thus moving the adlayer “away from percolation,” and the analogous behavior occurs for vacancy regions above 0.80 ML. However, in the crossover regime of 0.65–0.80 ML, the ramified network of filled regions is preserved and coarsens over several hours [Fig. 1(b)]. It is believed that a near-percolating structure such as this is necessary to support coarsening via edge running [8]. Ernst, Fabre, and Lapujoulade reported this effect at 0.5 ML for Cu/Cu(100) [8], in contrast to our observation of 0.65–0.80 ML. The contradiction is explained by the fact that they used low-temperature deposition to produce a quasi-random initial adlayer state (rather than one with large, compact islands). At 0.5 ML, this quasirandom state is much closer to the random “lattice percolation” value of about 0.6 ML, and contains clusters which are more highly ramified than does the initial state of our system at the same θ .

In summary, we have provided a comprehensive view of coarsening of Ag/Ag(100) adlayers. In particular, we find dominance of CD over OR in the coarsening of adatom islands up to 0.65 ML, and accurately model the kinetics using the known value of D . In contrast to simple intuition, we observe dramatic asymmetry between the diffusion and coarsening of vacancy islands at high θ , and of adatom islands at low θ . The location of the transition region between these two regimes at 0.65–0.80 ML, characterized by interconnected networks, is explained using concepts from correlated percolation theory.

This work is supported by NSF Grants No. CHE-9317660 and No. GER-9024358. Some equipment and all facilities are provided by the Ames Laboratory, which is operated for the U.S. Department of Energy by Iowa State University.

*Present address: Department of Chemistry, University of Iowa, Iowa City, IA 52242-1294.

- [1] C. Günther *et al.*, Ber. Bunsenges. Phys. Chem. **97**, 522 (1993).
- [2] H. Röder *et al.*, Nature (London) **366**, 141 (1993).
- [3] S.-L. Chang and P. A. Thiel, CRC Crit. Rev. Surf. Chem. **3**, 239 (1994).
- [4] T. L. Einstein, in *Chemistry and Physics of Solid Surfaces*, edited by R. Vanselow and R. Howe (Springer, Berlin, 1982), Vol. 4, p. 251.
- [5] J. A. Venables, Philos. Mag. **27**, 697 (1973), and references therein.
- [6] M. C. Bartelt and J. W. Evans, Surf. Sci. **298**, 421 (1993); Mater. Res. Soc. Symp. Proc. **312**, 255 (1993); J. Vac. Sci. Technol. **A12**, 1800 (1994).
- [7] M. Zinke-Allmang, L. C. Feldman, and M. H. Grabow, Surf. Sci. Rep. **16**, 377 (1992).
- [8] H.-J. Ernst, F. Fabre, and J. Lapujoulade, Phys. Rev. Lett. **69**, 458 (1992).
- [9] I. M. Lifshitz and V. V. Slyosov, J. Phys. Chem. Solids **19**, 35 (1961).
- [10] J. D. Gunton, M. S. Miguel, and P. S. Sahní, in *Phase Transitions and Critical Phenomena*, edited by C. Domb and J. L. Lebowitz (Academic Press, New York, 1983), Vol. 8, p. 267.
- [11] C. Chapon and C. R. Henry, Surf. Sci. **106**, 152 (1981).
- [12] S. Stoyanov and D. Kashchiev, in *Current Topics in Materials Science*, edited by E. Kaldis (North-Holland, Amsterdam, 1981), Vol. 7, p. 71, and references therein.
- [13] I. C. Oppenheim *et al.*, Science **254**, 687 (1991).
- [14] J. de la Figuera *et al.*, Solid State Commun. **89**, 815 (1994).
- [15] J.-M. Wen *et al.*, Phys. Rev. Lett. **73**, 2591 (1994).
- [16] M. V. Smoluchowski, Phys. Z. Sowjetunion **17**, 585 (1916).
- [17] E. Ruckenstein and B. Pulvermacher, J. Catal. **29**, 225 (1973).
- [18] F. Leyvraz, in *On Growth and Form*, edited by H. E. Stanley and M. Ostrowsky (Nijhoff, Boston, 1986).
- [19] M. N. Barber and B. W. Ninham, *Random and Restricted Walks* (Gordon and Breach, New York, 1970).
- [20] J.-M. Wen and P. A. Thiel (to be published).